

The weathering and element fluxes from active volcanoes to the oceans: a Montserrat case study

Morgan T. Jones¹, Deborah J. Hembury¹, Martin R. Palmer¹, Bill Tonge², W. George Darling³ & Susan C. Loughlin⁴

¹School of Ocean and Earth Science, University of Southampton, National Oceanography Centre, European Way, Southampton SO14 3ZH, UK

²Montserrat Water Authority, P.O. Box 324, Davy Hill, Montserrat, West Indies

³British Geological Survey, Maclean Building, Wallingford, Oxon OX10 8BB, UK

⁴British Geological Survey, West Mains Road, Edinburgh EH9 3LA, UK

Abstract The eruptions of the Soufrière Hills volcano on Montserrat (Lesser Antilles) from 1995 to present have draped parts of the island in fresh volcanoclastic deposits. Volcanic islands such as Montserrat are an important component of global weathering fluxes, due to high relief and runoff and high chemical and physical weathering rates of fresh volcanoclastic material. We examine the impact of the recent volcanism on the geochemistry of pre-existing hydrological systems and demonstrate that the initial chemical weathering yield of fresh volcanic material is higher than that from older deposits within the Lesser Antilles arc. The silicate weathering may have consumed 1.3% of the early CO₂ emissions from the Soufrière Hills volcano. In contrast, extinct volcanic edifices such as the Centre Hills in central Montserrat are a net sink for atmospheric CO₂ due to continued elevated weathering rates relative to continental silicate rock weathering. The role of an arc volcano as a source or sink for atmospheric CO₂ is therefore critically dependent on the stage it occupies in its life cycle, changing from a net source to a net sink as the eruptive activity wanes. While the onset of the eruption has had a profound effect on the groundwater around the Soufrière Hills center, the geochemistry of springs in the Centre Hills 5 km to the north appear unaffected by the recent volcanism. This has implications for the potential risk, or lack thereof, of contamination of potable water supplies for the island's inhabitants.

Keywords: Soufrière Hills volcano, Montserrat, Silicate weathering, CO₂ sequestration, Hydrology, Geochemistry

INTRODUCTION

The geochemistry of groundwater on active volcanic islands is of interest because of potential contamination of water supplies by volcanic ash leachates and magmatic volatiles (Johnston et al. 2000). Strong evidence exists for synergistic interactions between volcanism and groundwater, such that volcanic activity influences groundwater chemistry (Aiuppa et al. 2000; Varekamp 2008) and changing groundwater levels may trigger volcanic activity

(Matthews et al. 2002). Volcanic islands commonly have high relief and runoff and are comprised of easily weathered volcanic material (Eiriksdottir et al. 2008). Elevated mechanical and chemical weathering in volcanic terrains has been recognized as an important component in the transport of global dissolved load to the oceans (Rad et al. 2007) and therefore plays a significant role in the consumption of atmospheric CO₂ and the marine geochemical budgets of a variety of cations (Gaillardet et al. 1999; Dessert et al. 2003; Rad et al. 2006; Goldsmith et al. 2010).

Island arc products generally range from basaltic to dacitic in composition. The more silicic end of this spectrum, andesites and dacites, are viscous magmas that lead to explosive eruptions and the formation of lava domes. The long-lived deposits that comprise the bulk of island arc volcanoes are primary block-and-ash flow deposits and secondary lahar deposits, which fill drainages around the volcano and prograde as alluvial fans out to sea (Barclay et al. 2007). This mode of volcanism has important consequences for the subsequent weathering of material. The majority of unlithified deposits are extremely porous and permeable, such that much of the runoff is subsurface (Rad et al. 2007). This allows for elevated reaction rates between volcanic deposits and percolating fluids due to higher temperatures and longer water residence times.

Explosions, dome collapses, and venting produce significant amounts of tephra (airborne volcanic particles), which can be widely dispersed. Tephra deposition can also affect surface runoff as it sticks to vegetation, killing the leaves. This aids the subsequent erosion by precipitation through reduced canopy cover (Collins and Dunne 1986; Major and Mark 2006). Pumice flow (from eruption column collapse events) and tephra fallout deposits typically only last for days to weeks on volcanic arc islands, depending on the thickness of the deposits, the local relief, and the amount of precipitation.

We examined the impact of recent and sustained volcanism on the geochemistry of hydrologic systems on the Caribbean island of Montserrat, where there has been intense volcanic activity over the past decade. We aimed at determining silicate weathering rates on this andesitic volcano to compare with other islands in the Lesser Antilles arc.

FIELD AREA

The Soufrière Hills volcano, located in the southern part of the island of Montserrat in the Lesser Antilles (Fig. 1), is an andesitic stratovolcano that had been dormant since the seventeenth century. The island comprises three distinct volcanic massifs, the extinct northern Silver Hills (2.6–1.2 Ma) and Centre Hills (950–550 ka), and the active Soufrière Hills (170 ka to present) (Harford et al. 2002). The massifs are largely formed of andesite lava domes with aprons of volcanic breccias, representing mainly pyroclastic flow deposits and lahar deposits. The most recent eruption of the Soufrière Hills volcano commenced in 1995 and is ongoing. The current eruption is characterized by periodic lava-dome growth, dome collapse pyroclastic flows (block-and-ash flows), and vulcanian explosions, some of which generate pumice flows (e.g., Carn et al. 2004; Edmonds et al. 2006; Trofimovs et al. 2006). Over the 15 years of the current eruption, ~1 km³ of volcanic material has been erupted, with between 75% and 90% of material eventually deposited in the surrounding ocean (Trofimovs et al. 2006). Thick pyroclastic flow and lahar deposits have built up in valleys in the south of the island, extending across older alluvial fans and building new deltas (Barclay et al. 2007) (Fig. 1). The geochemical hydrology of Montserrat was studied prior to the recent volcanic activity in 1977 and 1991–1992 (Wright et al. 1976; Bath 1977; Chiodini et al. 1996). Sampling of the main Centre Hills springs was also carried out in August–September 2003, 8 years into the eruption (Davies and Peart 2003).

The soils on Montserrat are comparable to elsewhere in the Lesser Antilles and are predominantly Andosols. These soil formations can reach 70 m thick in the Lesser Antilles (Rad et al. 2007), although on Montserrat the soils are thinner due to the island's small size, steep topography, and relatively young age. As with Dominica (Goldsmith et al. 2010), these combined factors have restricted soil development. The soils are generally thicker and more deeply weathered towards the north of the island where older deposits outcrop. The dominance of coarse soils creates a porous surface, allowing water to percolate by infiltration. This creates soil aquifers in the central part of the island, with associated springs. Proximal to the volcano, subsurface water is more typified by groundwaters that have percolated through recent volcanoclastic deposits.

Rainfall is highest in the south and west of the island and lower in the north and east. The most extensive recent records are from the gauge at Hope (site 8) and show an average

rainfall of 1.72 m/year between 1999 and 2007. However, there is considerable inter-annual variability, such that total rainfall at Hope in 2007 was only 1.31 m, compared to 2.75 m in 2004 (Montserrat Water Authority, unpublished data). Average annual rainfall over the summit areas of Centre Hills and Soufrière Hills is estimated to be ~2.5 m/year (Davies and Peart 2003). There are no published evapotranspiration data for Montserrat, but in the thickly vegetated areas of Centre Hills, it is likely to be similar to the 30% of precipitation observed on the nearby islands of Martinique and Guadeloupe (Rad et al. 2007). Over the bare flanks of the volcano, water loss through evaporation will be closer to the open-water evaporation rates of 1.4–2.6 m/year measured on Montserrat by Bramble and Barragne-Bigot (1988). There is no perennial surface water runoff from the island, other than from streams fed directly by spring water, and these are currently confined to the Centre Hills area. Surface runoff does occur following periods of sustained high rainfall, as observed in the Belham valley during this study.

SAMPLING AND METHODS

Springs, surface runoff, and rivers were sampled and analyzed during a field investigation of Montserrat from 13th to 30th June 2008. At this time, the Soufrière Hills volcano had no lava extrusions following the end of the third episode of lava dome growth in early April 2007. There was no ash fall in the Centre Hills during the field investigation, although there was a permanent plume of gas. A total of 19 sites were sampled, with repeat sampling conducted at several locations (Fig. 1 and Table 1).

In Montserrat, the wet season lasts from June to November. Sampling at the end of the dry season increased the likelihood of detecting any volcanic influence in spring and surface waters. The prevailing wind is from the east and southeast, though occasionally from the south, such that deposition of volcanic gases and aerosols will largely affect areas to the west, northwest, and to a lesser extent the north of the Soufrière Hills volcano. The weather was mostly dry and sunny during the field investigation, apart from showers on the 20th and 23rd June and minor rainfall on the 26th June.

The springs in the western Centre Hills (sites 2–8) were sampled at source. These springs are the main source of potable water on the island and are enclosed to prevent detritus entering the pipes. The springs in the eastern Centre Hills (sites 12a, 12b, 15, and 16) are not currently

tapped nor cordoned off, allowing some direct input from atmospheric sources. Attempts were made to sample surface runoff wherever possible. Site 13 (Soldier Ghaut in the Centre Hills) is a stream with near-continuous surface runoff above 350-m elevation with an unknown source.

Around the volcano, intense rainfall sometimes instigates lahars, particularly in the Belham River valley. Site 14 (the location of the former Belham Bridge) and site 1 (the mouth of the Belham River) were sampled after heavy rains led to surface runoff. In addition, pits were dug into the volcanic deposits to reach the water table at sites 1, 9–11, and 17. These pits did not exceed 2-m depth and were left for 10 min prior to sampling to allow disturbed particulates to settle. The final sample locations were site 18 (Hot Pond), a thermal spring northwest of the former capital Plymouth, and site 19, a 115-m-deep borehole by the former Belham Bridge that is utilized by the Montserrat Water Authority.

Conductivity, pH, and temperature were measured in situ. Samples were collected in rinsed high-density polyethylene (HDPE) bottles and passed through 0.45- μm filters within a few hours of collection. The filtered waters were sub-sampled into 30-ml HDPE bottles for anion and Sr isotope analysis, into 60-ml HDPE bottles which were acidified to 1% by volume with sub-boiled Suprapure® HNO_3 for cation analysis, and into 100-ml glass bottles for $\delta_{18}\text{O}$, $\delta_{13}\text{C}$, and δD analysis. Alkalinity was measured as soon after collection as possible (under 3 h), using $3\text{MH}_2\text{SO}_4$ to titrate solutions. Element concentrations were analyzed at the National Oceanography Centre, Southampton, using inductively coupled plasma–mass spectrometer for cations and ion chromatography for anions. The precision of the individual concentrations is generally better than $\pm 5\%$. The $^{87}\text{Sr}/^{86}\text{Sr}$ ratios for each sample were measured using a VG Sector 54 thermal ionization mass spectrometer at Southampton. The samples were evaporated to dryness, taken up in 3 M HNO_3 , and run through Sr-spec columns. The purified Sr was then loaded onto outgassed Ta filaments. The samples were run at ^{88}Sr beam potentials of 2 V, and 150 ratios were collected using a multi-dynamic peak jumping routine. The ratios were normalized to an $^{86}\text{Sr}/^{88}\text{Sr}$ ratio of 0.1194. Twenty eight analyses of the NBS 987 standard yielded an average $^{87}\text{Sr}/^{86}\text{Sr}$ of 0.710256 ± 18 (2 SD). $\delta_{18}\text{O}$, $\delta_{13}\text{C}$, and δD were analyzed at the British Geological Survey, using standard methods. Analytical precisions were $\pm 0.1\%$, $\pm 0.2\%$, and $\pm 1\%$, respectively. Values of $\delta_{18}\text{O}$ and δD are expressed with respect to VSMOW and $\delta_{13}\text{C}$ with respect to VPDB. HCO_3^- concentrations were estimated by assuming that total alkalinity is carbonate alkalinity and using the following equations:

$$[HCO_3^-] = \frac{2 \times 10^{-pH} \cdot CA}{2(k + 10^{-pH})} \quad (1)$$

$$k = \frac{[H^+] \cdot [CO_3^{2-}]}{[HCO_3^-]} = 4.84 \times 10^{-11} \quad (2)$$

where *CA* denotes carbonate alkalinity and *k* is the equilibrium constant for HCO₃⁻ (or the second dissociation constant for carbonic acid).

RESULTS

The analytical results in Table 2 give a charge balance within ±10% of the total cation charge and most balance within ±5%, suggesting that there is no significant contribution to the geochemical composition of the waters from any species not included in Table 2. The cation and anion concentrations of the samples are depicted in ternary diagrams in Fig. 2 (after Giggenbach 1988). The Sr isotope, δ₁₈O, δD, and δ₁₃C data are listed in Table 3.

Centre Hills

Chiodini et al. (1996) analyzed the Olveston (site 5), Lawyers (site 3), and Killiekrankie (site 6) springs from Centre Hills in 1991–1992, and Davies and Peart (2003) analyzed most of the Centre Hills springs in 2003. Hence, it is possible to make a limited comparison of the groundwater geochemistry in the Centre Hills before and since the onset of the present volcanic activity. The Centre Hills waters fall into the spring classification of neutral Ca–Mg–HCO₃ type (Giggenbach 1988), and they all plot slightly above the meteoric δD–δ₁₈O line (MWL) (Fig. 3), as indeed do the spring samples of Davies and Peart (2003) and Chiodini et al. (1996). The “deuterium excess” (i.e., y-axis intercept) depends largely on humidity in the moisture source area and can fluctuate around the global mean of +10 (e.g., Clark and Fritz 1997). The spring waters are unmodified rainfall, as indicated by the O and H isotope data. However, comparing the 2008 data with that of Davies and Peart (2003) shows a consistent difference running sub-parallel to the MWL (Fig. 4). This shows a change in the isotopic balance of the groundwater, which may be seasonal or secular. These isotopic shifts

imply that the groundwaters are not well mixed and therefore that storage and subsurface residence times are relatively short.

The Centre Hills waters data lie on a mixing line between the average $^{87}\text{Sr}/^{86}\text{Sr}$ of local andesitic rocks (Cooper 2005) and rainwater (Rad et al. 2007) on a Sr isotope mixing diagram (Fig. 5). The $\delta_{13}\text{C}$ values are typical of groundwater with no carbonate weathering. A mixture of CO_2 derived from decaying organic matter in soil ($\delta_{13}\text{C}\approx-25\text{‰}$) and atmospheric CO_2 ($\delta_{13}\text{C}\approx-7.9\text{‰}$) (Faure 1986) (Fig. 6) explain these data best, which is typical of short-lived interaction between meteoric waters and rocks in shallow aquifers (Freeze and Cherry 1979). It is possible that magmatic volatiles from Soufrière Hills volcano leaked into the Centre Hills aquifer. Of the species measured in all three studies, F/Cl ratios are more likely to record any such input due to the high relative ratio of these halogens in magmatic fluids compared to seawater-derived sources. The average F/Cl is lower in the 2008 and 2003 samples than in the 1991–1992 samples (Table 4). In addition, As and Se concentrations were below detection limits (2 and 1 nmol/l, respectively) in the 2008 samples (Table 2), which are commonly elevated in fluids of magmatic origin. Hence, we find no evidence of any magmatic volatile input into the Centre Hills groundwaters.

Abundant ash deposition and continuous gas emissions from the Soufrière Hills volcano have taken place since 1995. Most of the tephra and gas are carried to the west and northwest of the volcano, occasionally affecting the southwestern flanks of the Centre Hills. Occasional major lava dome collapses and vulcanian explosions have led to significant ash falls and acid rain over most of the Centre Hills. Rainwater pH values as low as 2.7 have been recorded as far north as Lawyers (site 3) as a result of high emissions of HCl, SO_2 , and other acids from the volcano (MVO unpublished data). Deposition of easily weathered tephra and acids over Centre Hills could also lead to an increase in cation concentrations in the groundwaters if recharge took place by filtration through ash layers. However, the small-scale nature of the tephra deposits, coupled with the high relief and precipitation, means the tephra residence times are usually confined to weeks. The short residence time is further enhanced by the loss of vegetation from ash deposition and increased surface runoff (Major and Mark 2006). The Ca/Cl, Mg/Cl, and SO_4/Cl molar values are essentially indistinguishable for the confined springs pre- and syn-eruption (Table 4). The SO_4/Cl molar ratios are only slightly higher than the seawater ratio of 0.052 that would be expected in meteoric water uncontaminated by volcanic emissions on a small island. This suggests that the infiltration of volcanically

derived SO_4 in the recharge water is very limited and there is no observed enhancement of weathering since the onset of the eruption.

The unconfined springs measured in 2008—namely Corbett (site 12), Ginger Ground (site 16), and Bottomless Ghaut (site 15)—have significantly higher SO_4/Cl ratios (0.113–0.126, 0.080, and 0.260, respectively) than the other Centre Hills springs. This may suggest a small contribution from surface runoff influenced by volcanically derived SO_4 to these waters. Overall, however, it appears that the compositions of the Centre Hills springs are largely unaffected by the volcanic activity that is occurring only 5 km south of their geographical center.

The flow rates of the Centre Hills springs are sensitive to rainfall, with a 4–6-month delayed response (Davies and Peart 2003). The Killiekrankie (site 6), Lawyers (site 3), and Olveston (site 5) springs were all sampled on three separate occasions, over the course of 17 years, at times of very different flow rates (Fig. 7). In particular, the 2003 samples were taken after a period of prolonged regional drought (Davies and Peart 2003). Despite this, the concentrations of the individual species and the elemental ratios remain relatively constant (Table 4), suggesting that the groundwater chemistry is close to equilibrium with a constant secondary mineral assemblage. On a stability diagram (Fig. 8), the Centre Hills data form a vertical array on the kaolinite–smectite line, suggesting that the groundwater composition is close to equilibrium with these minerals.

An alternative method is to take the mass balance approach to determining the weathering signature (Table 5). First, the contribution due to rainwater is subtracted from the average spring water compositions, on the assumption that all the Cl^- is derived from meteoric water (the discussion above demonstrates that the contribution from volcanic volatiles and acid rain is minor) and that the other species are present in seawater ratios. Next, it is assumed that all the remaining Na^+ is balanced by whole-rock weathering, with the contributions of the other cations derived from average andesite from the Centre Hills (Zellmer et al. 2003). This approach yields a remarkably good agreement between the calculated and observed water compositions (within the uncertainties of the average whole-rock compositions; Zellmer et al. 2003). The exception is an over-prediction in the amount of dissolved K^+ that would be expected, which might suggest that the smectite predicted from the stability calculations is K rich.

Belham Valley

The Belham Valley catchment lies at the boundary between the Centre Hills and the NW-aligned Garibaldi and St. Georges Hills. Two production boreholes have been sunk close to the site of the old Belham Bridge and cased to a depth of ~57 m below the surface. Water was pumped from below this depth with sustainable yields of ~4,250 and 1,625 l/min in 2004 (Hydrosource Associates Inc. 2004). The shallower of two aquifers is thought to lie within a ~15-m-thick layer of coarse gravel and weathered pebbles that are buried beneath 58 m of volcanic breccia and lahar deposits of undetermined age (Hydrosource Associates 2004). The more productive of the two wells was sampled in this study (site 19).

Lahars frequently flow down the Belham Valley after intense rain (Barclay et al. 2007), with some filling the entire width of the valley (~200 m) and producing standing waves up to 2 m in height (MVO weekly report, 21st May 2004). During this study, surface runoff was generated after 1 day of sustained rainfall that was a few centimetres deep and lasted for ~3 h. This was sampled close to the borehole at the location of the former Belham Bridge (site 14).

In most respects, the composition of the Belham Valley borehole water is similar to that of the Centre Hills springs. It has slightly lower pH (6.78 compared to a range 6.94–7.68) and is slightly enriched in elements such as Na, Mg, Si, Cl, K, Ca, Fe, Rb, and Sr (Table 2). On the K/H₂ versus SiO₂ discrimination diagram (Fig. 8), it plots well within the smectite stability field, which together with the higher total dissolved salts (TDS), is consistent with the borehole tapping a deeper, longer residence-time reservoir than the Centre Hills springs. The baseline (i.e., well-mixed, longterm mean), $\delta_{18}\text{O}$, and δD isotopic compositions for the southwest side of the island are probably best represented by this site (Fig. 3). The F/Cl (1.02×10^{-3}) of the borehole water is well within the range exhibited by the Centre Hills springs, but the $\delta_{13}\text{C}$ value lies on a mixing line between average Centre Hills spring waters and typical geothermal fluids (Fig. 6). This suggests that there is some small hydrothermal input into the aquifer (at the time of sampling), consistent with the findings of Younger (2006).

The composition of the Belham valley surface runoff (site 14) is clearly distinct from the springs and borehole. The TDS is approximately one third of that of the Centre Hills springs, while the Sr isotope plot (Fig. 5) suggests that the surface runoff is simply a mixture of spring water and meteoric water. However, the relatively low pH and ternary diagrams (Fig. 2) reveal that this is not the case. On the secondary mineral assemblage stability diagram (Fig.

8), the Belham surface runoff composition plots on the gibbsite–kaolinite boundary, and this is also reflected in the high dissolved Al concentration (16 $\mu\text{mol/l}$) compared to the spring waters (generally $<1 \mu\text{mol/l}$) (Table 2). The slight effect of geothermal fluids found at depth in the Belham catchment is absent from the surface runoff. Therefore, if it is assumed that all the Cl^- is derived from rainfall, and the other ions in meteoric water are present in seawater ratios; then a correction due to this source can be made. The chemical composition of the surface runoff water due to weathering can then be calculated. When this calculation is applied to the Sr isotope ratios, then the $^{87}\text{Sr}/^{86}\text{Sr}$ of the weathering component is calculated to be 0.7037—very close to the value of 0.7036 for average Montserrat volcanic rocks (Cooper 2005). This calculation also suggests that relatively little of volcanically derived HCl was deposited on the flanks during this study (if less Cl^- is ascribed to a rainwater source, the calculated $^{87}\text{Sr}/^{86}\text{Sr}$ of the rock component would be higher). Edmonds et al. (2003) have shown that HCl emissions are dependent on magma ascent rate, so the lack of magma extrusion before or during this study suggests low emissions of HCl at this time. While Cl^- is scavenged very quickly by dry and wet depositional processes and would therefore increase closer to the vent, the lack of elevated Cl^- in the Belham catchment (1–5 km from the vent) adds weight to this assertion. Table 5 does, however, suggest that the chemical composition of the surface runoff water is significantly impacted by deposition of sulfate in its watershed, consistent with the relatively constant emissions of SO_2 from Soufrière Hills regardless of extrusion rate. This is reflected in both the low pH and the fact that SO_4 is the major anion balancing the cation charge after accounting for the meteoric water contribution, suggesting that sulfuric acid was the main weathering agent in the Belham surface runoff water during this field study.

The relatively dilute nature of the surface runoff waters compared to the spring waters makes it more difficult to specify the composition of the phases undergoing weathering. Nevertheless, it is clear that the balance of cations is distinct from that observed in the Centre Hills springs, with Na^+ being by far the dominant cation (Table 2). This suggests that there is selective dissolution of Na-rich phases. The major Na-bearing mineral phase in Soufrière Hills volcanic rocks is plagioclase (Humphreys et al. 2009), but studies of feldspar weathering consistently show preferential dissolution of anorthite relative to albite (Blum and Stillings 1995). Hence, the most likely source of the high Na^+ in the surface runoff waters is preferential dissolution of volcanic glass, which commonly has higher Na/Ca ratios than whole rock in fresh volcanic material (Cashman 1992). Glass is uncommon in dome rocks

and block-and-ash flow deposits but comprises a significant proportion of the fine tephra (Bonadonna et al. 2002). Such fine material is rapidly transported through the Belham catchment by fluvial processes, so in the absence of eruptive activity prior to the study, most of this fine glass would have already been transported offshore. Therefore, the glass contributing the excess Na^+ is likely to be predominantly from pumice transported into the catchment by occasional pumice flows in 2007 and frequent lahars.

Shallow groundwater

Recently, deposited volcanic materials such as pyroclastic flow and lahar deposits are generally highly permeable, such that surface water flow is restricted to periods of high rainfall. With this in mind, we carried out a reconnaissance survey that involved digging shallow (1–2 m) pits at the mouths of gullies (Ghauts) on the western flank of the Soufrière Hills volcano (Fig. 1). Most of the pits had to be dug within ~100 m of the shore to reach the water table, so inevitably they contain a major seawater component—either as a result of surface spray or mixing of seawater with the groundwater (Fig. 2, Table 2)—making it difficult to discern the weathering signature.

The exception is provided by the sample from the mouth of Gingoës Ghaut (site 17) which has relatively high pH (Table 2). The Cl^- concentration is lower than the other shallow groundwater samples but is still significantly higher than observed in the Centre Hills springs or the Belham Valley surface runoff sample. This may reflect seawater contamination, it may arise from concentration of the dissolved load by the high evaporation/rainfall ratio on the barren slopes of the volcano during the dry season (Bramble and Barragne-Bigot 1988), or it may reflect acid rain deposition from the volcanic plume. Acid rain at Lower Amersham, the closest sample site to Gingoës, had a pH range 2.55 to 3.90 in June 1996–June 1997. The average Cl^- concentration of 3.48 ± 0.98 mmol/l (Smithsonian Institution 1997) is indistinguishable from that measured in the Gingoës groundwater in 2008. However, studies of atmospheric deposition around Mt. Etna have revealed that the flux of dissolved Na, Ca, Mg, and K is derived almost entirely from sea spray (Aiuppa et al. 2006). If all the Cl^- in the Gingoës groundwater was ascribed to deposition from the volcanic plume, together with the associated concentrations of SO_4 and F^- , there would be a net positive charge imbalance in the remaining ions. Alternatively, if all the Cl^- is ascribed to a marine origin (either directly from

seawater mixing with the groundwater or indirectly via meteoric water), there would be a negative charge imbalance. The best charge balance is achieved if 25% of the Cl⁻ is ascribed to deposition from the volcanic plume and 75% is ascribed to a direct (through a seawater component in the groundwater) or indirect seawater source (through sea spray and/or meteoric water) (Table 5).

The relative concentrations of the cations derived from weathering compared to their concentrations in average Soufrière Hills rocks (Zellmer et al. 2003) indicate that Na⁺ is relatively high, which suggests that there is incongruent dissolution of the rock and/or there is significant retention of the other cations in secondary minerals. Evidence in favor of the latter is provided by the presence of the Gingoos sample within the smectite stability field (Fig. 8), but extensive Ca²⁺, Mg²⁺, and K⁺ uptake into smectite is required to balance the Na⁺ derived from congruent dissolution of average Soufrière Hills rocks. Hence, it is possible that, as suggested for the Belham Valley surface runoff sample, the relatively high Na⁺ concentrations in the groundwater results from preferential dissolution of Na-rich volcanic glass.

The dissolved F⁻ concentrations in Gingoos subsurface water are considerably higher than observed in either the Centre Hills springs or the Belham Valley lahar waters (Table 2). The head of Gingoos Ghaut drains the upper slopes of Chances Peak, close to the site of steam vents associated with the present phase of volcanic activity. Hence, the elevated F⁻ levels may reflect some magmatic volatile input into the groundwater. This is supported by the $\delta_{13}\text{C}$ value (-4.42‰), which clearly indicates a dominant magmatic component for the dissolved inorganic carbon in the groundwaters (Fig. 6). The cations derived from weathering are almost exactly equally balanced between HCO₃⁻ (4.82 meq/l) and SO₄²⁻ (4.78 meq/l). This suggests that half of the weathering signature is derived from leaching by sulfuric acid, formed from oxidation and solution of H₂S and SO₂ in magmatic gases, and half from magmatic CO₂. Sulfuric acid forms up to 7–40% of the anhydrous gas in fumaroles, and CO₂ forms 59–92% of the anhydrous phase of fumarole gases from Soufrière Hills (Chiodini et al. 1996; Hammouya et al. 1998).

Geothermal water

The Hot Pond spring (site 18) situated in Amersham northwest of Plymouth displays element concentrations of the neutral Na–Cl type. These are characterized by medium–high

temperatures ($<90^{\circ}\text{C}$) and display chemical compositions that are indicative of medium- to high enthalpy geothermal reservoirs (Ellis and Mahon 1977). The equilibrium temperatures and Cl^- contents of the pure geothermal liquid involved in the origin of the Hot Pond waters are predicted to be $245\text{--}250^{\circ}\text{C}$ and $665\text{--}690\text{ mmol/l}$, respectively (Chiodini et al. 1996). The Hot Pond springs are relatively depleted in SO_4 and Mg with respect to seawater while enriched in Ca, suggesting vigorous and sustained element exchange with country rock. The likely cause of this thermal spring is due to seawater-hot rock interaction along a zone of crustal weakness. The role of seawater is clearly indicated here by the $^{87}\text{Sr}/^{86}\text{Sr}$ ratio (0.705677), which is intermediate between that of Montserrat volcanic rocks (0.7036) and seawater (0.70916) (Fig. 5). Hot Pond is situated close to the NW trending zone that also features the Soufrière Hills volcano and St. George's Hill and Garibaldi Hill to the north of Plymouth. This zone of crustal weakness has acted as an upflow path for rising magma (Wadge and Isaacs 1988) and has allowed seawater to percolate to depth and react with the hot rocks. The lack of pronounced enrichment of volcanic volatiles (such as SO_4 and F) suggests that there is minimal input of magmatic water into the Hot Pond aquifer. However, the $\delta_{13}\text{C}$ value (-5.25‰) suggests that there is a significant contribution of gaseous magmatic CO_2 to the geothermal system (Fig. 6), while the relatively low dissolved inorganic carbon (DIC) and low pH (5.40) also suggest that the fluid has undergone boiling at depth with secondary loss of CO_2 from the fluids.

The Hot Pond spring has been sampled on at least five occasions between 1976 and 2008 (Bath 1977; Chiodini et al. 1996; MVO unpublished data, 1998; Younger 2006; this study). The data are of variable completeness and quality, but they do show some consistent trends (Fig. 9). Since the onset of the most recent phase of volcanic activity in 1995, there have been clear falls in the temperature, pH, and Li concentration of the fluids and a rise in the SO_4 concentrations. The temperature of the springs can vary by $>10^{\circ}\text{C}$ on a weekly basis (R. Syers, personal communication), so the measured temperature change (Fig. 9) is not necessarily indicative of a decrease in the flow of hot water to the surface. Both the decrease in pH and increase in SO_4 concentrations could be due to a relative increase in the proportion of gases derived from sub-surface phase separation and/or a response to the increase in average SO_2 emissions from the volcano. The ultimate cause of these changes cannot be discerned from these data alone. Figure 10 shows a $\delta_{18}\text{O}\text{--Cl}$ plot for the various samples for Hot Ponds. The three samples taken between 1976 and 2008 lie on a mixing line between seawater with a slight ^{18}O shift and well-mixed meteoric waters of Belham borehole type,

marked as cool groundwater. The good fit of these data again suggests that the contribution of magmatic water is negligible.

DISCUSSION

Weathering fluxes

A recent survey of groundwater and surface water geochemistry on three volcanic tropical islands (Martinique and Guadeloupe in the Lesser Antilles and Réunion in the Indian Ocean) led Rad et al. (2007) to conclude that weathering in these environments contributes 25–30% of the global dissolved load transported to the oceans, despite the fact that they only represent 9% of the global land area. These high weathering rates arise from the fact that unlithified volcanic rocks are very porous, causing much of the runoff to be subsurface where reaction rates are accelerated by higher temperatures and longer water residence times. In addition, younger volcanic rocks have not had time to develop the thick mantle of weathered material that is characteristic of tropical volcanic islands with high rainfall. A recent study by Goldsmith et al. (2010) on the island of Dominica highlighted the importance of crystallinity and the age of the parent material on the concentrations of solutes in runoff. Their study concludes that silicate weathering yields and subsequent CO₂ consumption in andesitic terrains are comparable to basaltic terrains.

Detailed hydrologic models are not available for Montserrat. Nevertheless, the recent deposits around the volcano and the thick soils of the Centre Hills are relatively permeable, such that runoff is largely confined to subsurface flow during the dry season, while significant rainfall creates surface runoff during the wet season once the infiltration rates are exceeded. The average rainfall over the ~25 km² of the Centre Hills area is ~1.5 m/year (Davies and Peart 2003) and if we assume that evapotranspiration is similar to the 30% of precipitation observed on the nearby islands of Martinique and Guadeloupe (Rad et al. 2007), this yields an annual water flux of 26×10^6 m³/year. After adjusting the average spring water compositions for the rainwater component, this yields a minimum average silicate weathering flux of ~70 t/km² per year (in the absence of any significant weathering during surface runoff). This is considerably higher than the global average silicate weathering rate of ~7 t/km² per year (Gaillardet et al. 1999), comparable to the surface runoffs of nearby islands of

Dominica (6–106 t/km² per year; Goldsmith et al. 2010) and Martinique and Guadeloupe (100–120 t/km² per year; Rad et al. 2006), but lower than 290–1,090 t/km² per year for subsurface weathering on Martinique and Guadeloupe (Rad et al. 2007). This discrepancy with regard to subsurface weathering likely reflects the fact that the Centre Hills massif is an extinct volcano and has an age of 950–550 ka (Harford et al. 2002), whereas the areas studied by Rad et al. (2007) include historically active volcanoes and recent unlithified or partially lithified channel-fill volcanic deposits.

Calculation of weathering rates over Soufrière Hills is speculative due to the absence of hydrologic data on the active volcano. Nevertheless, if the data for Gingoès Ghaut are representative of groundwater compositions in Soufrière Hills, then some estimates can be made. Gingoès Ghaut drains an area of ~2.5 km². Rainfall is higher over this area (~2.5 m/year; Davies and Peart 2003), but the absence of vegetation means that evapotranspiration is also likely to be higher (Bramble and Barragne-Bigot 1988). If, for the purposes of illustration, we assume that evapotranspiration is double that observed over Centre Hills (i.e., ~60%), then the runoff in Gingoès Ghaut is 2.5×10^6 m³/year, and the average weathering flux is ~600 t/km² per year. This figure is comparable with the 1,080 t/km² per year measured for subsurface weathering on Martinique (Rad et al. 2007). The total surface area covered by volcanic deposits on Montserrat varies depending on the state of volcanic activity and the subsequent erosion. Figure 1 shows the pyroclastic flow deposits, lahar deposits, and pumice flow deposits and excludes tephra deposits, such as long-lived tephra deposits on St Georges Hill and in the headwaters of Belham Valley. Both pumice flow deposits and airfall deposits are relatively short-lived, such that the degree of volcanoclastic coverage varies from season to season. For the purposes of the following calculations, it is assumed that the average coverage at the time of sampling is ~30 km², which yields a total silicate weathering flux from the Soufrière Hills volcano of 18×10^3 t/year.

CO₂ consumption during weathering in Centre Hills is $\sim 1.7 \times 10^6$ mol/km² per year compared to a global average due to silicate weathering of 0.6×10^6 mol/km² per year, with the $\delta_{13}\text{C}$ values indicating that all of this CO₂ derived directly from the atmosphere with no discernable magmatic input. Extrapolation of the Gingoès Ghaut data (site 17) yields a CO₂ consumption rate of 4.8×10^6 mol/km² per year or 150×10^6 mol/year over the ~30 km² covered by recent volcanic material (Fig. 1). Based on an average SO₂ flux of 400 t/day and a CO₂/SO₂ ratio of ~3.5, Hammouya et al. (1998) calculated the average CO₂ flux from the volcano during dome growth between 1995 and 1997 to be 1,400 t/day (32×10^6 mol/day). Daily average SO₂ fluxes

from the Soufrière Hills volcano have been relatively constant at ~500 t/day up until 2005 and have since increased. The current CO₂/SO₂ ratio is unknown, but if the 1996 figures are considered representative of average SO₂ and CO₂ degassing rates during at least the early years of the eruption, then only ~1.3% of the annual CO₂ flux from the volcano was consumed by silicate weathering on the island at that time.

There are no published data that explicitly describe CO₂ degassing rates from Soufrière Hills prior to the present phase of activity, but using the hot spring and fumarole data of Chiodini et al. (1996) and following the approach of Taran (2009), it was likely to have been of the order of ~1 t/day (0.23×10^6 mol/day). Approximately 20% of this CO₂ was dissolved in the hot spring waters that ultimately flowed into the ocean. If weathering rates prior to the recent phase of activity were similar to those in Centre Hills today, then the Soufrière Hills massif would have been close to being in balance regarding the CO₂ source from the volcano and the CO₂ sink from weathering.

Hence, the role of an andesitic arc volcano, such as Soufrière Hills, as a source or sink for atmospheric CO₂ depends critically on the stage it occupies in its life cycle. During the pre-eruptive phase when volatiles are rising to the surface, there appears to be a fine balance between CO₂ uptake due to weathering and loss to the atmosphere from degassing. During the active phase of volcanism, magmatic degassing far outweighs the enhanced weathering signature. Once the volcano becomes dormant or extinct, magmatic degassing ceases and the enhanced weathering of volcanic rocks (relative to continental silicate rock weathering) results in the volcanic rocks acting as a sink for atmospheric CO₂. The behavior of CO₂ during the transition from an active to a dormant or extinct phase is complicated by the uncertain role played by CO₂ degassing of plutonic rocks in arc environments and the difficulty in measuring passive CO₂ degassing rates (Marty and Tolstikhin 1998). Resolution of this problem will require extensive studies of CO₂ degassing and weathering fluxes from arc volcanoes, covering a spectrum of ages, tectonic regimes, and weathering environments. However, the undoubted importance of arc volcanism in defining the composition of modern and ancient atmospheric CO₂ levels (Kerrick 2001) requires us to solve this problem if we are to develop a deeper understanding of the evolution of global climate.

CONCLUSIONS

This field study demonstrates the importance of weathering of fresh volcanic material as a sink of atmospheric CO₂. The high silicate weathering rates from both the extinct Centre Hills and the active Soufrière Hills volcanoes confirm that weathering of young andesitic terrains has a disproportionate effect on the consumption of CO₂ with respect to the land surface area. This carbon sequestration through elevated weathering is initially dwarfed by the CO₂ emissions from the active Soufrière Hills volcano, such that silicate weathering consumes a predicted 1.3% of the CO₂ released by magmatic degassing. However, as the sub-aerial exposure times of volcanic centers greatly exceed that of the active life span of the volcano, the extent to which arc volcanoes are overall sinks or sources of atmospheric CO₂ is uncertain. However, at any given time, the stage of the volcano's life cycle is critically important in the balance between a source and sink of CO₂. The importance of lithification of volcanic deposits may also become important on a timescale of 100,000s of years.

The lack of magmatic influence on the springs situated in the Centre Hills suggests that the geochemical influence of recent volcanic activity is completely restricted to the south of the island, implying a narrow conduit for rising magmatic volatiles and fluids beneath the Soufrière Hills volcano. The sporadic coverings of tephra and acids on the Centre Hills appear to have had no significant impact on the covered potable springs, suggesting that Montserrat's current water supply is not in danger of contamination from the ongoing volcanic activity. However, the observed change in the isotopic balance of the groundwater since 2003 implies that these waters are not well mixed. These changes may well be seasonal, but given the lack of explosive activity prior to this study, this may have had an effect on the apparent lack of volcanic signature from infiltration of acids as all tephra deposited in the Centre Hills had been removed for some time prior to the study. The boreholes situated in the Belham valley (site 19) suggest some interaction with magmatic gases, and monitoring of the geochemical signature of these waters may provide a valuable insight into the variations in the release of magmatic gases into the proximal aquifer.

Acknowledgements This work was funded by the National Environment Research Council (NERC). The authors would like to thank the staff of the Montserrat Volcano Observatory for their valuable assistance during excursions into the exclusion zone, particularly Nico Fournier, Thomas Christopher, and Racquel Tappy Syers. Reuel Lee and Mervin Tuitt of the Montserrat Water Authority are thanked for their able assistance in sample collection. Many thanks are due to Johan Varekamp and Jérôme Gaillardet for constructive reviews and to Pierre Delmelle for handling this manuscript.

References

- Aiuppa A, Allard P, D' Alessandro WD, Michel A, Parello F, Treuil M, Valenza M (2000) Mobility and fluxes of major, minor and trace metals during basalt weathering and groundwater transport at Mt. Etna volcano (Sicily). *Geochim Cosmochim Acta* 64:1827–1841
- Aiuppa A, Bellorno S, Brusca L, D' Alessandro W, Di Paola R, Longo M (2006) Major-ion bulk deposition around an active volcano (Mt. Etna, Italy). *Bull Volcanol* 68:255–265
- Barclay J, Alexander J, Susnik J (2007) Rainfall-induced lahars in the Belham Valley, Montserrat, West Indies. *J Geol Soc Lond* 164:815–827
- Bath AH (1977) Summary of hydrochemical data from the geothermal area in Montserrat, West Indies. British Geological Survey Report, WD/OS/77/2
- Blum AE, Stillings LL (1995) Feldspar dissolution kinetics. *Rev Mineral* 31:291–351
- Bonadonna CB, Mayberry GC, Calder ES et al (2002) Tephra fallout in the eruption of Soufrière Hills Volcano, Montserrat. In: Druitt TH, Kokelaar BP, Young SR (eds) *The eruption of Soufrière Hills Volcano, Montserrat, from 1995 to 1999*, vol 21, Geological Society Memoir. Geological Society of London, London, pp 483–516
- Bramble BL, Barragne-Bigot P (1988) Hydrogeology map of Montserrat: explanatory note. UN Project RLA/82/023. United Nations, Water in Small Islands of the Caribbean Project, joint project work of UNDTCD and COHI/CMI
- Carn SA, Watts RB, Thompson G, Norton GE (2004) Anatomy of a lava dome collapse: the 20 March event at Soufriere Hills Volcano, Montserrat. *J Volcanol Geoth Res* 131:241–264
- Cashman KV (1992) Groundmass crystallization of Mount St. Helens dacite, 1980–1986: a tool for interpreting shallow magmatic processes. *Contrib Mineral Petrol* 109:431–449
- Chiodini G, Cioni R, Frullani A, Guidi M, Marini L, Prati F, Raco B (1996) Fluid geochemistry of Montserrat Island, West Indies. *Bull Volcanol* 58:380–392
- Clark ID, Fritz P (1997) *Environmental isotopes in hydrogeology*. CRC/Lewis, Boca Raton
- Collins BD, Dunne T (1986) Erosion of tephra from the 1980 eruption of Mount St. Helens. *Geol Soc Am Bull* 97(7):896–905
- Cooper R (2005) Sr–Nd–Pb isotope evolution of Montserrat since 300 ka. M.Sc. thesis, University of Southampton

- Davies J, Peart RJ (2003) A review of the groundwater resources of central and northern Montserrat. British Geological Survey Commissioned Report CR/03/257C
- Dessert C, Dupre B, Gaillardet J, Francois LM, Allegre CJ (2003) Basalt weathering laws and the impact of basalt weathering on the global carbon cycle. *Chem Geol* 202:257–273
- Di Napoli R, Aiuppa A, Bellomo S, Brusca L, D'Alessandro W, Candela EG, Longo M, Pecoraino G, Valenza M (2009) A model for Ischia hydrothermal system: evidences from the chemistry of thermal groundwaters. *J Volcanol Geoth Res* 186:133–159
- Edmonds M, Oppenheimer C, Pyle DM, Herd RA (2003) Rainwater and ash leachate analysis as proxies for plume chemistry at Soufrière Hills Volcano, Montserrat. *Geol Soc Lond Spec Publ* 213:203–218
- Edmonds M, Herd RA, Strutt MH (2006) Tephra deposits associated with a large lava dome collapse, Soufriere Hills Volcano, Montserrat, 12–15 July 2003. *J Volcanol Geoth Res* 153(3–4):313–330
- Eiriksdottir ES, Louvat P, Gislason SR, Oskarsson N, Hardardottir J (2008) Temporal variation of chemical and mechanical weathering in NE Iceland: evaluation of a steady-state model of erosion. *Earth Planet Sci Lett* 272:78–88
- Ellis AJ, Mahon WAJ (1977) *Chemistry and geothermal systems*. Academic, New York
- Faure G (1986) *Principles of isotope geology*. Wiley, New York
- Freeze RA, Cherry JA (1979) *Groundwater*. Prentice Hall, Englewood Cliffs
- Gaillardet J, Dupre B, Louvat P, Allegre CJ (1999) Global silicate weathering and CO₂ consumption rates deduced from the chemistry of large rivers. *Chem Geol* 159:3–30 *Bull Volcanol*
- Giggenbach WF (1988) Geothermal solute equilibria. Derivation of Na–K–Mg–Ca geothermometers. *Geochim Cosmochim Acta* 52:2749–2765
- Goldsmith ST, Carey AE, Johnson B Met al (2010) Stream geochemistry, chemical weathering and CO₂ consumption potential of andesitic terrains, Dominica, Less Antilles. *Geochim Cosmochim Acta* 74:85–103
- Hammouya G, Allard P, Jean-Baptiste P, Parello F, Semet MP, Young SR (1998) Pre- and syn-eruptive geochemistry of volcanic gas from Soufrière Hills of Montserrat, West Indies. *Geophys Res Lett* 25:3685–3688
- Harford CL, Pringle MS, Sparks RSJ, Young SR (2002) The volcanic evolution of Montserrat using ⁴⁰Ar/³⁹Ar geochronology. In: Druitt TH, Kokelaar BP, Young SR (eds) *The eruption of Soufrière Hills Volcano, Montserrat, from 1995 to 1999*, vol 21, Geological Society Memoir. Geological Society of London, London, pp 93–113
- Humphreys MCS, Christopher T, Hards V (2009) Microlite transfer by disaggregation of mafic inclusions following magma mixing at Soufrière Hills volcano, Montserrat. *Contrib Mineral Petrol* 157:609–624

- Hydrosource Associates Inc. (2004) Groundwater exploration and development report for the development of two production wells. Technical report
- Johnston DM, Houghton BF, Neall VE, Ronan KR, Paton D (2000) Impacts of the 1945 and 1995–1996 Ruapehu eruptions New Zealand: an example of increasing societal vulnerability. *Geol Soc Am Bull* 112:720–726
- Kerrick DM (2001) Present and past nonanthropogenic CO₂ degassing from the solid earth. *Rev Geophys* 39:565–585
- Le Friant A, Harford CL, Deplus C et al (2004) Geomorphological evolution of Montserrat (West Indies): importance of flank collapse and erosional processes. *J Geol Soc Lond* 161:147–160
- Major JJ, Mark LE (2006) Peak flow responses to landscape disturbances caused by the cataclysmic 1980 eruption of Mount St. Helens, Washington. *Geol Soc Am Bull* 118:938–958
- Marty B, Tolstikhin IN (1998) CO₂ fluxes from mid-ocean ridges, arcs and plumes. *Chem Geol* 145:233–248
- Matthews AJ, Barclay J, Carn S, Thompson G, Alexander J, Herd R, Williams C (2002) Rainfall-induced volcanic activity on Montserrat. *Geophys Res Lett*. doi:10.1029/2002GL014863
- Rad S, Louvat P, Gorge C, Gaillardet J, Allegre CJ (2006) River dissolved and solid loads in the Lesser Antilles: new insight into basalt weathering processes. *J Geochem Explor*. doi:10.1016/j.gexplo.2005.08.063
- Rad S, Allegre CJ, Louvat P (2007) Hidden erosion on volcanic islands. *Earth Planet Sci Lett* 262:109–124
- Smithsonian Institution (1997) Soufrière Hills. *Bull Glob Volcanism Netw* 22:2–4
- Taran YA (2009) Geochemistry of volcanic and hydrothermal fluids and volatile budget of the Kamchatka-Kuril subduction zone. *Geochim Cosmochim Acta* 73:1067–1094
- Trofimovs J, Amy L, Boudon G et al (2006) Submarine pyroclastic deposits formed at the Soufrière Hills volcano, Montserrat (1995–2003): what happens when pyroclastic flows enter the ocean? *Geology* 34(7):549–552
- Varekamp JC (2008) The volcanic acidification of glacial Lake Caviahue, Province of Neuquen, Argentina. *J Volcanol Geoth Res* 178:184–196
- Wadge G, Isaacs MC (1988) Mapping the volcanic hazard from Soufrière Hills volcano, Montserrat, West Indies, using an image processor. *J Geol Soc Lond* 145:541–551
- Wright EP, Murray KH, Bath AH (1976) Geothermal investigations in Montserrat, May 1976. British Geological Survey Report WD/OS/76/12
- Younger PL (2006) Preliminary assessment of the technical feasibility and likely costs of the development of geothermal power generation on the island of Montserrat, East Caribbean. Report to Montserrat Utilities Ltd., 37 pp
- Zellmer GF, Hawkesworth CJ, Sparks RSJ et al (2003) Geochemical evolution of the Soufrière Hills volcano, Montserrat, Lesser Antilles volcanic arc. *J Petrol* 44:1349–1374

Table 1 Sample details

Sample	Location	Type	Alt. (m)	Latitude N	Latitude W	Date
SW	Belham River Shore	Seawater	0	16° 44' 28.5"	062° 13' 60.0"	23-Jun-08
1a	Belham River Shore	Subsurface	1	16° 44' 28.7"	062° 13' 59.3"	13-Jun-08
1c	Belham River Shore	Pool	1	16° 44' 28.7"	062° 13' 59.3"	13-Jun-08
1d	Belham River Shore	Runoff	1	16° 44' 28.7"	062° 13' 59.3"	20-Jun-08
1e	Belham River Shore	Runoff	1	16° 44' 28.7"	062° 13' 59.3"	20-Jun-08
1f	Belham River Shore	Runoff	1	16° 44' 28.7"	062° 13' 59.3"	23-Jun-08
1g	Belham River Shore	Runoff	1	16° 44' 28.7"	062° 13' 59.3"	23-Jun-08
1h	Belham River Shore	Runoff + SW	1	16° 44' 28.7"	062° 13' 59.3"	23-Jun-08
2a	Forgarthy Spring	Spring	309	16° 46' 08.3"	062° 12' 27.1"	14-Jun-08
2c	Forgarthy Spring	Spring	309	16° 46' 08.3"	062° 12' 27.1"	24-Jun-08
3a	Lawyer Spring	Spring	174	16° 45' 36.8"	062° 12' 57.7"	14-Jun-08
3b	Lawyer Spring	Spring	174	16° 45' 36.8"	062° 12' 57.7"	24-Jun-08
4a	Quashie Spring	Spring	245	16° 45' 30.2"	062° 12' 57.1"	14-Jun-08
4b	Quashie Spring	Spring	245	16° 45' 30.2"	062° 12' 57.1"	24-Jun-08
5a	Olveston Spring	Spring	261	16° 45' 21.0"	062° 12' 49.4"	14-Jun-08
5b	Olveston Spring	Spring	261	16° 45' 21.0"	062° 12' 49.4"	24-Jun-08
6a	Killiekrankie Spring	Spring	324	16° 44' 33.7"	062° 11' 55.6"	15-Jun-08
6b	Killiekrankie Spring	Spring	324	16° 44' 33.7"	062° 11' 55.6"	25-Jun-08
7a	Monkey Spring	Spring	339	16° 44' 30.4"	062° 11' 51.3"	15-Jun-08
7b	Monkey Spring	Spring	339	16° 44' 30.4"	062° 11' 51.3"	25-Jun-08
8a	Hope Spring	Spring	294	16° 45' 06.9"	062° 12' 43.8"	15-Jun-08
8b	Hope Spring	Spring	294	16° 45' 06.9"	062° 12' 43.8"	24-Jun-08
9a	Kinsale-Aymer's Ghaut	Subsurface	5	16° 41' 52.0"	062° 12' 56.2"	17-Jun-08
9b	Kinsale-Aymer's Ghaut	Subsurface	5	16° 41' 52.0"	062° 12' 56.2"	26-Jun-08
10	Government House	Subsurface	7	16° 42' 05.8"	062° 13' 07.8"	17-Jun-08
11	Plymouth-Fort Ghaut	Subsurface	11	16° 42' 33.8"	062° 13' 28.5"	17-Jun-08
12a	Corbett Springs (b)	Spring	281	16° 45' 00.1"	062° 11' 13.6"	18-Jun-08
12b	Corbett Springs (a)	Spring	275	16° 44' 58.7"	062° 11' 15.7"	18-Jun-08
13	Soldier Ghaut	Riverine	400	16° 45' 52.7"	062° 12' 06.5"	22-Jun-08
14	Belham Bridge	Runoff	281	16° 44' 28.8"	062° 13' 05.4"	23-Jun-08
15	Bottomless Ghaut	Spring	379	16° 45' 59.9"	062° 11' 29.4"	25-Jun-08
16	Ginger Ground	Spring	429	16° 46' 07.7"	062° 11' 31.7"	25-Jun-08
17	Gingoes Ghaut	Subsurface	2	16° 41' 27.4"	062° 12' 36.8"	26-Jun-08
18	Hot Pond	Spring	6	16° 43' 07.8"	062° 13' 46.3"	26-Jun-08
19	Belham Borehole	Borehole	281	16° 44' 29.0"	062° 13' 05.4"	30-Jun-08

Table 2 Sample geochemical data

Sample	Region	pH	Temp. °C	Alk. meq/l	Li nM	B nM	NO ₃ nM	F nM	Na mM	Mg mM	Al nM	Si mM	SO ₄ nM	Cl nM	K nM	Ca nM	V nM	Cr nM	Mn µM	Fe µM	Ni nM	Cu nM	As nM	Se nM	Br µM	Rb µM	Sr µM	Ba µM
SW		8.02	28.2	2.38	31.3	441.2	nd	46.6	526.96	67.68	5.6	0.06	28.56	574.39	12.79	12.86	123.9	8.6	0.25	0.22	124	10.5	340.8	1,272.8	660.15	1.58	90.38	0.11
1a	Belham	6.69	28.5	na	0.4	14.2	0.8	20.7	5.08	2.42	1.0	0.75	2.53	8.03	0.27	2	36	nd	97.84	79.91	7.5	0.3	45.4	20.5	7.93	0.19	3.98	0.15
1c	Belham	6.4	30	na	1.2	86.7	5.3	27	70.61	7.44	nd	0.53	4.88	88.07	1.31	3.47	33.6	0.3	203.14	304.4	49.6	1.6	101.8	299.3	98.02	0.7	10.16	0.87
1d	Belham	4.29	33.5	0.06	1.6	7.7	30.7	53.6	2.05	0.6	230.2	0.24	3.91	1.91	0.16	2.36	19.5	0.5	67.09	3.45	42.4	24.9	nd	nd	1.45	0.13	4.19	0.24
1e	Belham	6.04	29.2	0.32	0.8	9.5	15.3	18.7	3.23	1.31	1.2	0.53	3.64	3.19	0.16	2.17	15.6	nd	113.22	91.36	25.6	1.7	19.2	nd	2.81	0.11	3.39	0.13
1f	Belham	4.25	27.1	na	1.3	7.1	nd	29.5	2.72	0.62	149.8	0.22	2.22	3.2	0.14	1.48	8	nd	80.36	2.15	22.3	19.4	nd	3.2	3.59	0.1	2.75	0.2
1g	Belham	4.68	27.2	na	1.6	11.6	0.3	31.6	4.03	1.25	8.9	0.64	5.21	6.52	0.23	3.93	11.5	nd	172.39	149.37	59.5	5.5	8.2	5.48	0.17	7.04	0.33	
1h	Belham	7.79	27.8	2.22	24.3	350.9	nd	56.2	409.43	53.2	59.9	0.22	21.35	460.97	9.82	10.42	126	5.6	23.83	0.1	99	11.2	410.3	1,484.30	540.66	1.27	73.15	0.29
2a	Centre	7.68	23.6	1.68	0.2	5.5	3.5	1.3	1.58	0.46	1	0.53	0.07	1.23	0.03	0.34	191.5	4.1	0.06	0.09	nd	2.4	nd	nd	2.67	0.01	0.73	0.01
2c	Centre	7.45	23.2	1.55	0.2	4.8	8.1	1.2	1.34	0.43	nd	0.49	0.07	1.1	0.03	0.34	162.9	2.6	0.04	0.01	nd	1.6	nd	nd	2.4	0.01	0.71	nd
3a	Centre	7.14	23.5	na	0.1	3.9	14.1	1.3	1.14	0.38	nd	0.49	0.05	0.97	0.03	0.37	168.8	2.1	0.06	0.01	nd	1.1	nd	nd	2.03	0.02	0.7	nd
3b	Centre	7.53	24	1.48	0.1	3.5	0.3	0.7	1.15	0.38	nd	0.48	0.05	0.99	0.02	0.37	163.4	1.5	0.05	0.02	nd	1.3	nd	1.38	0.01	0.69	0.01	nd
4a	Centre	7.35	23.5	na	0.1	3.5	22.4	0.7	1.13	0.38	1.8	0.51	0.05	0.99	0.03	0.38	180.3	1.2	1.28	14.16	nd	3.8	nd	1.74	0.02	0.72	nd	nd
4b	Centre	7.25	23.5	1.51	0.1	3.4	8.5	0.9	1.11	0.38	0.1	0.51	0.05	0.99	0.03	0.38	171.1	2.1	0.05	0.01	nd	1.3	nd	2.11	0.02	0.72	nd	nd
5a	Centre	7.06	23.4	na	0.1	3.5	19.6	0.6	1.15	0.39	nd	0.5	0.05	0.92	0.02	0.39	128	3.3	0.01	0.01	nd	1.1	nd	1.87	0.02	0.75	0.01	nd
5b	Centre	6.94	23.4	1.55	0.1	3.5	4.3	0.7	1.15	0.39	nd	0.5	0.06	1.01	0.03	0.4	126	4	0.02	0.04	nd	1.3	nd	2.21	0.02	0.75	0.02	nd
6a	Centre	7.37	26	na	0.2	3.8	29.2	0.8	1.26	0.37	nd	0.54	0.07	1.14	0.03	0.42	199.7	nd	0.01	0.01	nd	0.3	nd	2.03	0.02	0.75	nd	nd
6b	Centre	7.34	26	1.51	0.2	3.8	17	1.6	1.25	0.37	3.6	0.54	0.07	1.15	0.03	0.42	203	0.3	0.01	0.01	nd	0.6	nd	2	0.02	0.74	nd	nd
7a	Centre	7.23	26.4	na	0.2	3.6	8.6	0.7	1.32	0.36	nd	0.53	0.08	1.18	0.02	0.41	183.2	nd	0.01	0.01	nd	0.3	nd	2.28	0.01	0.77	0.01	nd
7b	Centre	7.14	26.3	1.45	0.2	3.6	0.6	0.8	1.33	0.36	nd	0.53	0.08	1.18	0.02	0.41	196.3	nd	nd	nd	nd	0.3	nd	2.37	0.01	0.77	0.01	nd
8a	Centre	7.56	23.2	na	0.1	3.6	35.4	0.8	1.13	0.46	nd	0.56	0.06	1.09	0.03	0.47	228.1	1.2	0.01	nd	nd	0.3	nd	2.02	0.02	0.83	nd	nd
8b	Centre	7.48	23.4	1.74	0.2	4.1	12.3	0.8	1.32	0.51	nd	0.57	0.09	1.34	0.03	0.46	277.4	0.9	nd	nd	nd	0.3	nd	2.46	0.02	0.85	0.01	nd
9a	Plymouth	4.06	33.3	0.1	7.8	92	33.9	131.7	71.91	8.5	624.9	1.63	8.6	77.45	2.1	2.54	39.7	4	40.59	14.25	91.5	131.2	51.4	193.3	127.88	0.58	10.4	0.08
9b	Plymouth	4.13	27.7	na	1.4	12.2	173.4	178.2	1.43	0.94	376.2	0.65	1.37	2.6	0.19	1.58	10.3	5.2	37.46	0.7	44.1	11.8	nd	nd	3.29	0.12	1.65	0.05
10	Plymouth	4.14	33.2	na	7.7	65.5	16	114	37.43	5.41	473.7	1.94	8.12	40.95	1.21	6.05	35.6	1.5	127.47	249.79	135.4	111.1	nd	8.5	95.74	0.32	7.25	0.05
11	Plymouth	6.32	38.3	1.55	15.3	99.4	16.5	131.2	58	5.05	2.2	1.24	4.53	61.05	1.81	3.48	74.6	1.8	3.77	0.04	53.7	15.9	60.7	49.9	102.49	0.6	8.97	0.07
12a	Centre	7.31	26.3	2	0.1	5	12.5	2	1.62	0.47	nd	0.46	0.16	1.44	0.02	0.63	107.2	nd	0.12	0.01	nd	1.4	nd	3	0.01	0.97	nd	nd
12b	Centre	7.59	27	1.97	0.1	4.5	19.9	2.2	1.63	0.37	nd	0.44	0.18	1.39	0.02	0.63	107	nd	nd	nd	nd	0.2	nd	2.49	0.01	0.94	nd	nd
13	Centre	7.39	26.9	0.87	0	3	nd	2.4	0.86	0.23	0	0.42	0.21	0.77	0.04	0.33	33.5	nd	0.03	nd	nd	0.5	nd	1.06	0.02	0.62	0.01	nd
14	Belham	4.85	25.3	0.06	0.3	0.6	6.2	3.4	0.26	0.02	15.9	0.05	0.08	0.2	0.03	0.05	5	nd	2.14	0.58	nd	0.9	nd	0.16	0.02	0.12	0.07	nd
15	Centre	7.64	24.3	1.74	0	2.8	nd	1.3	1.12	0.38	3.2	0.74	0.25	0.95	0.03	0.61	31.1	nd	0.37	0.11	nd	0.3	nd	1.27	0.02	1.28	0.01	nd
16	Centre	7.14	24	2.19	0.1	3.8	0.1	2.9	1.73	0.43	nd	0.96	0.11	1.39	0.02	0.6	107.1	1.8	0.11	0.3	nd	0.2	nd	2.16	0.01	1.22	0.01	nd
17	Gingoes	6.25	32.1	4.83	1.6	38.8	245.6	46.6	9.4	1.08	6.2	1.23	2.6	3.48	0.45	0.42	99	2.4	0.27	0.22	5.5	5.4	34.4	7.44	0.1	0.19	0.02	nd
18	Hot Pond	5.40	43.5	0.97	526.2	1,125.8	5.5	33.6	185.3	12.37	13.6	2.21	1.97	296.38	14.59	35	76.3	2.1	467.98	126.11	390	16.1	1,386.8	571.1	357.22	13.7	179.9	11.6
19	Belham BH	6.78	31.5	3.16	0.7	12	35.9	2.1	2.43	0.96	nd	1.62	0.13	2.02	0.11	0.74	374.2	nd	0.13	1.1	9.7	0.6	nd	2.12	0.11	1.22	nd	nd

na samples not analyzed nd denotes concentrations below detection

Table 3 Isotope data of oxygen, hydrogen, carbon (all in per mill), and strontium (ratio) in selected samples

Sample	Region	$\delta^{18}\text{O}$	δD	$\delta^{13}\text{C}$	$^{87}\text{Sr}/^{86}\text{Sr}$
SW	na	na	na	na	0.70916
1d	Belham	-4.28	-21.7	-18.00	na
1e	Belham	na	na	na	0.70585
1g	Belham	na	na	na	0.70506
2a	Centre	na	na	na	0.70510
2c	Centre	-3.31	-13.7	-20.22	0.70472
3a	Centre	-3.25	-11.6	-19.41	0.70439
4a	Centre	-3.21	-12.7	-20.65	0.70442
5a	Centre	-3.26	-11.3	-19.62	0.70441
6a	Centre	-2.88	-9.7	-21.88	0.70435
7a	Centre	-2.83	-8.4	-24.61	0.70438
8a	Centre	-3.28	-10.5	-18.84	0.70446
9a	Plymouth	-2.76	-10.2	-9.60	0.70865
9b	Plymouth	na	na	na	0.70627
10	Plymouth	-2.34	-6.2	-12.21	0.70803
11	Plymouth	-2.53	-9.1	-10.04	0.70794
12a	Centre	-3.29	-10.3	-20.72	0.70428
12b	Centre	-3.14	-11.0	-20.15	0.70404
13	Centre	-2.76	-5.7	-15.59	0.70500
14	Belham	na	na	na	0.70516
15	Centre	-3.12	-8.2	-15.58	0.70454
16	Centre	-2.79	-8.2	-16.91	0.70464
17	Gingoes	-2.07	-4.5	-4.42	0.70861
18	Hot Pond Belham	-0.19	-7.1	-5.24	0.70568
19	BH	-3.21	-12.3	-10.41	0.70479
<i>na</i>	not analyzed				

Table 4 Summary of geochemical time series of Centre Hills springs

	Mg/Cl	Ca/Cl	SO₄/Cl	F/Cl (x10³)
Mar 1991 ^a	0.37	0.38	0.071	2.43
Aug–Sep 2003 ^b	0.36	0.39	0.071	1.28
Jun 2008 ^c	0.36	0.38	0.067	0.92

^aChiodini et al. (1996)

^bDavies and Peart (2003)

^cThis study. Data reported as molar ratios

Table 5 Summary of major element concentrations before subtraction of rain water component for selected samples

	Na	Ca	Mg	K	HCO₃	Cl	SO₄	F
Av. CH springs	1.347	0.438	0.412	0.025	1.642	1.181	0.087	0.92
Minus rain	0.335	0.416	0.297	0.005	1.639	0	0.031	0.78
Minus W-R	0.000±0.023	-0.001±0.042	0.054±0.049	-0.119±0.018	-0.015			
Av CH rock	1.09±0.07	1.36±0.14	0.79±0.04	0.40±0.06				
Belham lahar	0.264	0.049	0.025	0.025	0.06	0.196	0.076	3.44
Minus rain	0.096	0.046	0.006	0.021	0.06	0	0.066	3.42
Gingoes	9.4	0.422	1.082	0.451	4.83	3.48	2.6	47
Acid rain	6.91	0.367	0.799	0.397	4.82	3.48±0.98	0.31±0.05	77±1
Minus (25% plume + 75% sw)	0	2.39	27					
Av SSH rock	0.98±0.15	1.75±0.27	1.13±0.27	0.37±0.12				

Dissolved concentrations are in millimoles per liter, except F in micromoles per liter.

Acid rain composition from Smithsonian Institution (1997)

CH centre Hills, SSH South Soufriere Hills, SW seawater

Figure captions

Figure 1. Map of Montserrat, depicting the deposits from the Soufrière Hills volcano and the locations of samples collected in this study. Topographic and bathymetric data were collected by Le Friant et al. (2004).

Figure 2. Ternary diagrams showing the relative abundance by mass of **a** anions and **b** cations in the collected samples (field descriptors after Giggenbach (1988)). Gray-shaded areas denote the general fumarole compositions from Chances and Gages Peak (the sites of the subsequent eruptions) in 1991/1992 (Chiodini et al. 1996). Centre Hills data are ringed with a *black circle* with outliers labelled.

Figure 3. Oxygen and hydrogen isotopic ratios for the cool and thermal waters in Montserrat. SMOW standard mean ocean water, MWL meteoric water line.

Figure 4. A comparison of $\delta^{18}\text{O}$ and $\delta^2\text{H}$ variations from the Centre Hills springs between 2003 (Davies and Peart 2003) and this study (2008).

Figure 5. $^{87}\text{Sr}/^{86}\text{Sr}$ ratios versus $1/\text{Sr}$ for selected samples. The precipitation values for Guadeloupe are from Rad et al. (2006). Three end members exist: water–rock interaction, atmospheric input (rain), and seawater contamination. The average $^{87}/^{86}\text{Sr}$ ratio in Montserrat rocks is 0.7036 (Cooper 2005).

Figure 6. Carbon isotopic composition of DIC in Montserrat waters versus concentration of DIC in waters. Open squares = Centre Hills spring waters, solid square = Belham Valley bore hole, open circle = Gingoies Ghaut groundwater, cross = Hot Springs. The gray band shows the $\delta^{13}\text{C}$ of typical magmatic gases (Hammouya et al. 1998; Di Napoli et al. 2009).

Figure 7. Water flow rates for Killiekrankie, Olveston, and Lawyers springs in Centre Hills (Montserrat Water Authority, unpublished data). *Arrows* indicate sampling dates.

Figure 8. Stability diagram for secondary mineral assemblages at 25°C. *Open squares* = Centre Hills spring waters, *solid square* = Belham Valley bore hole, *solid circle* = Belham Valley lahar, *open circle* = Gingoies Ghaut groundwater.

Figure 9. Variation in chemistry and temperature of Hot Pond spring geothermal water (Bath 1977; Chiodini et al. 1996; MVO unpublished data, 1998; Younger 2006; this study). The *arrows* mark the onset of the most recent phase of volcanic activity.

Figure 10. A $\delta^{18}\text{O}$ –Cl plot for the various samples for Hot Pond spring (site 18) (Bath 1977; Chiodini et al. 1996; this study). The mixing line originates from cool groundwaters of Belham borehole type (site 19).

Figure 1

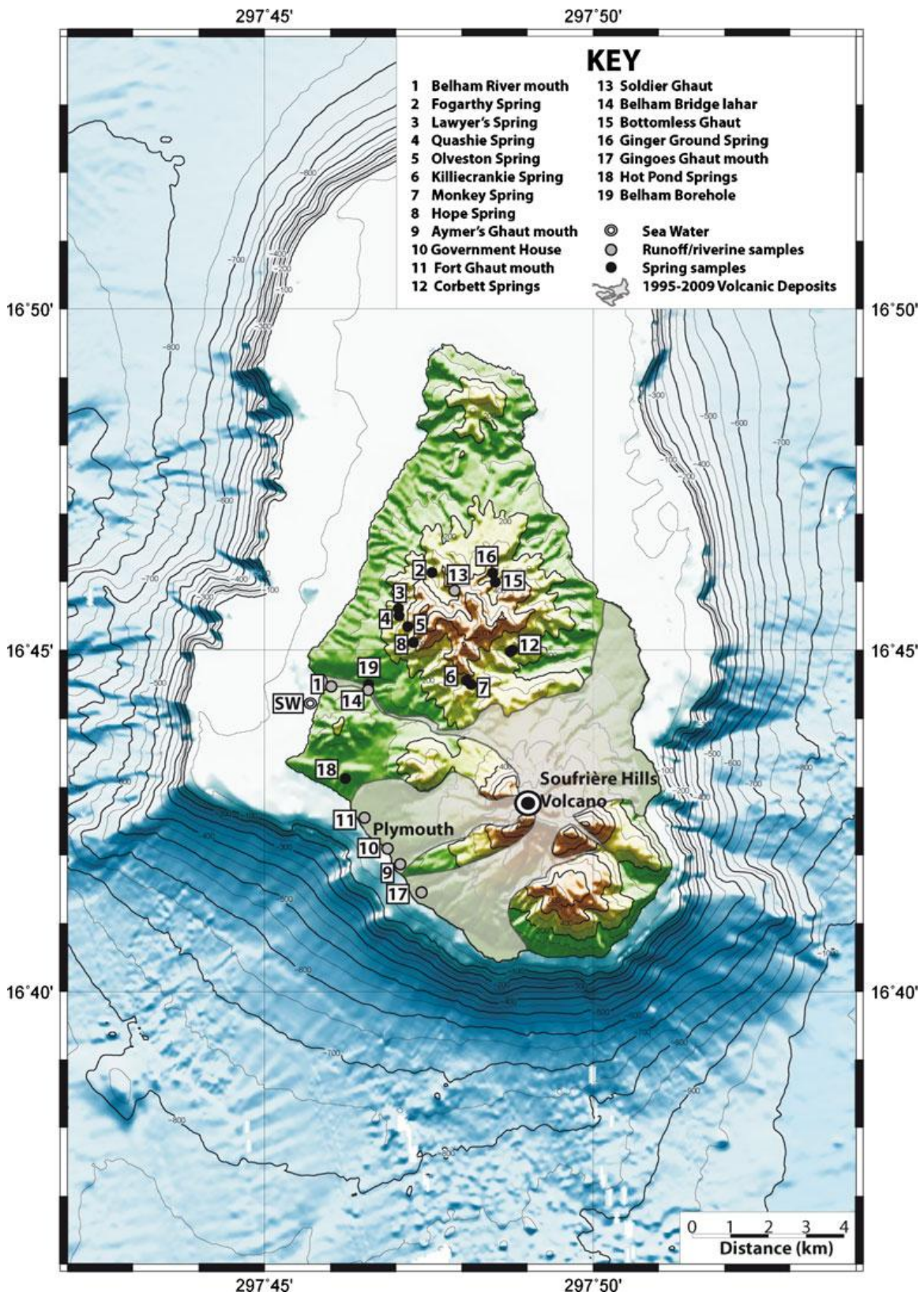


Figure 2

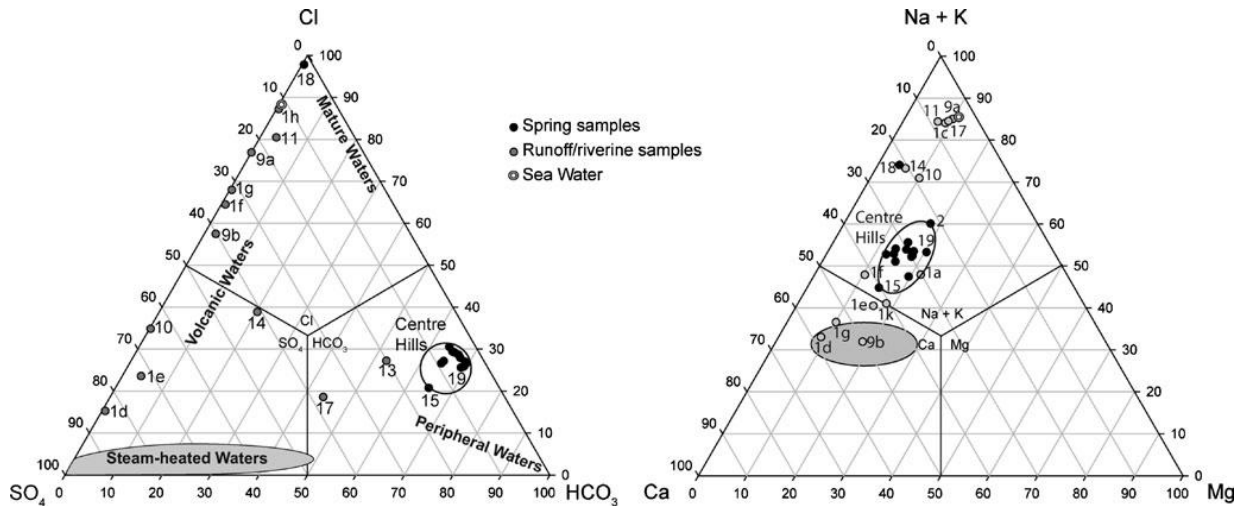


Figure 3

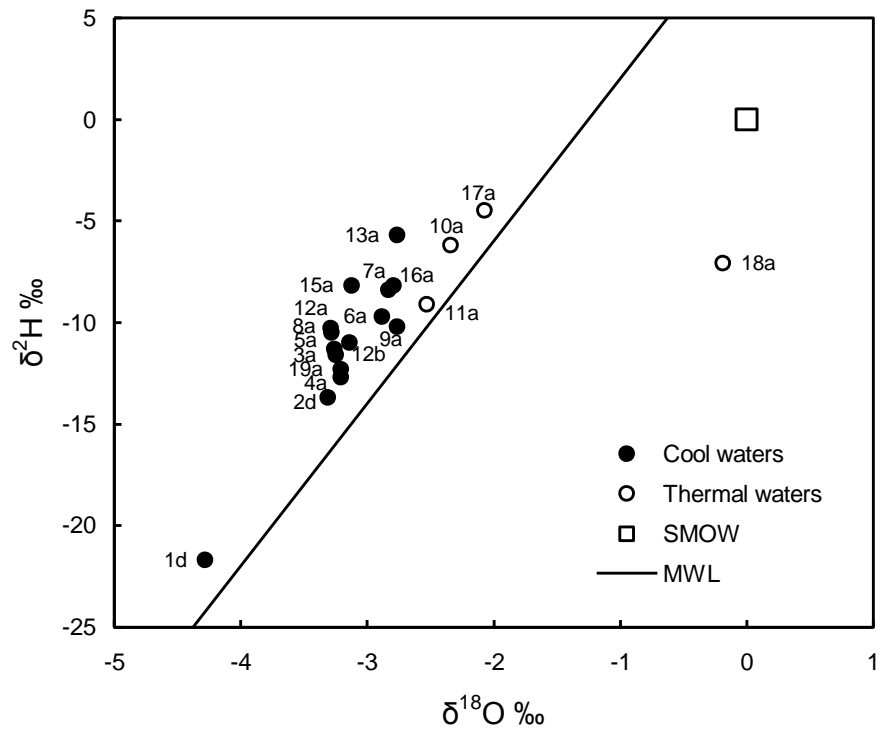


Figure 4

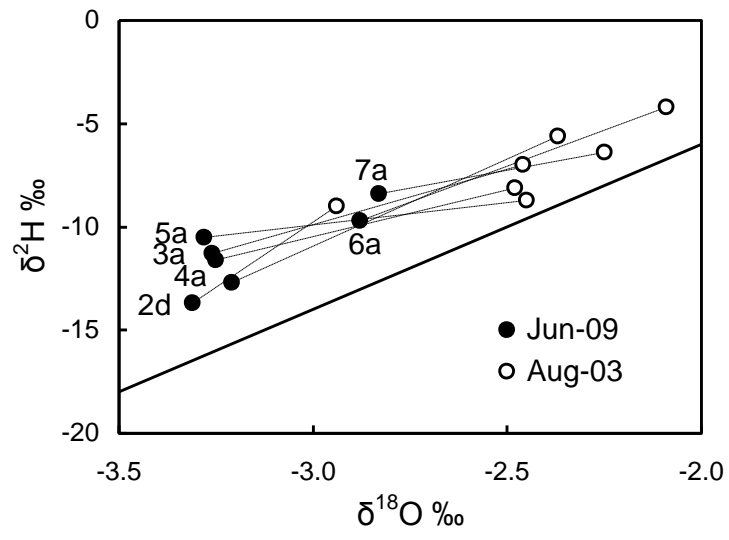


Figure 5

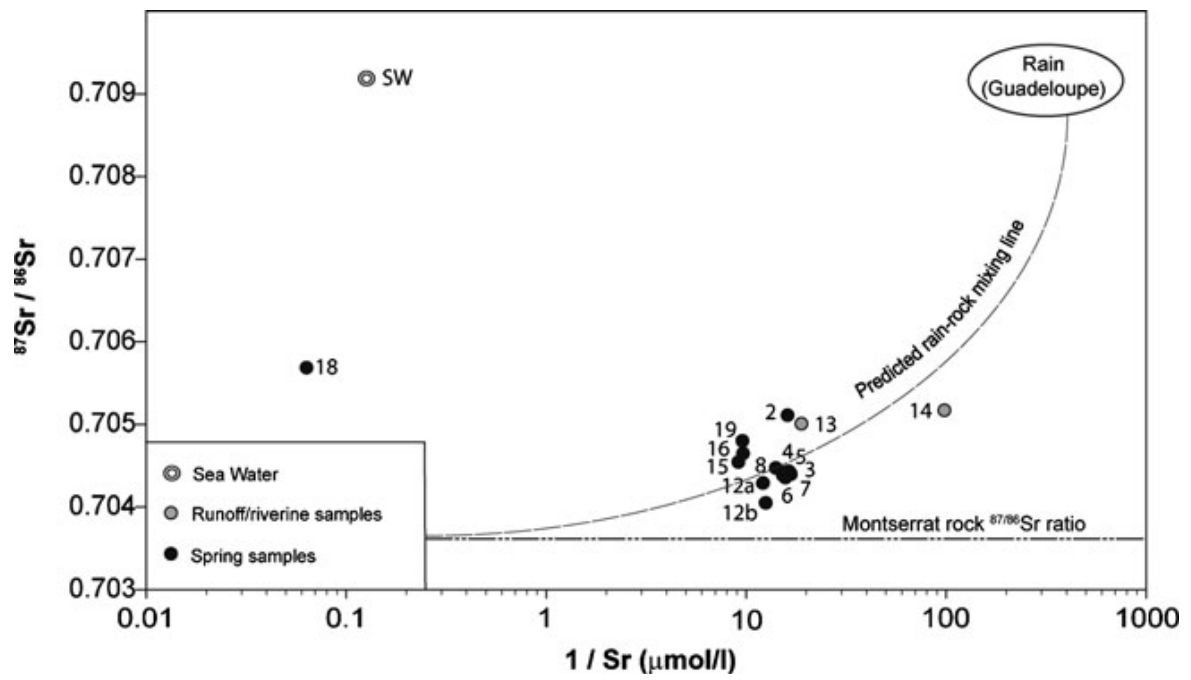


Figure 6

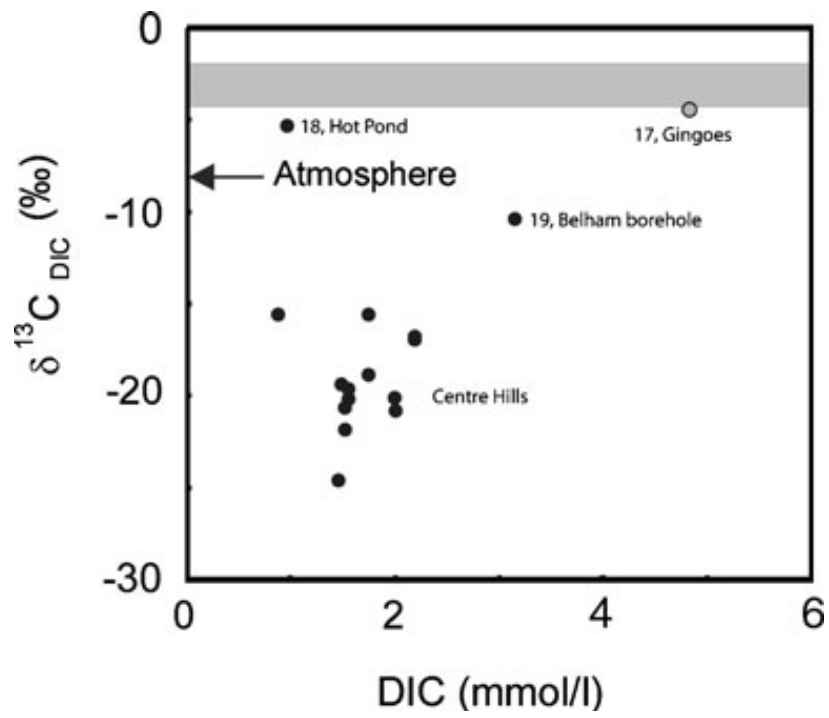


Figure 7

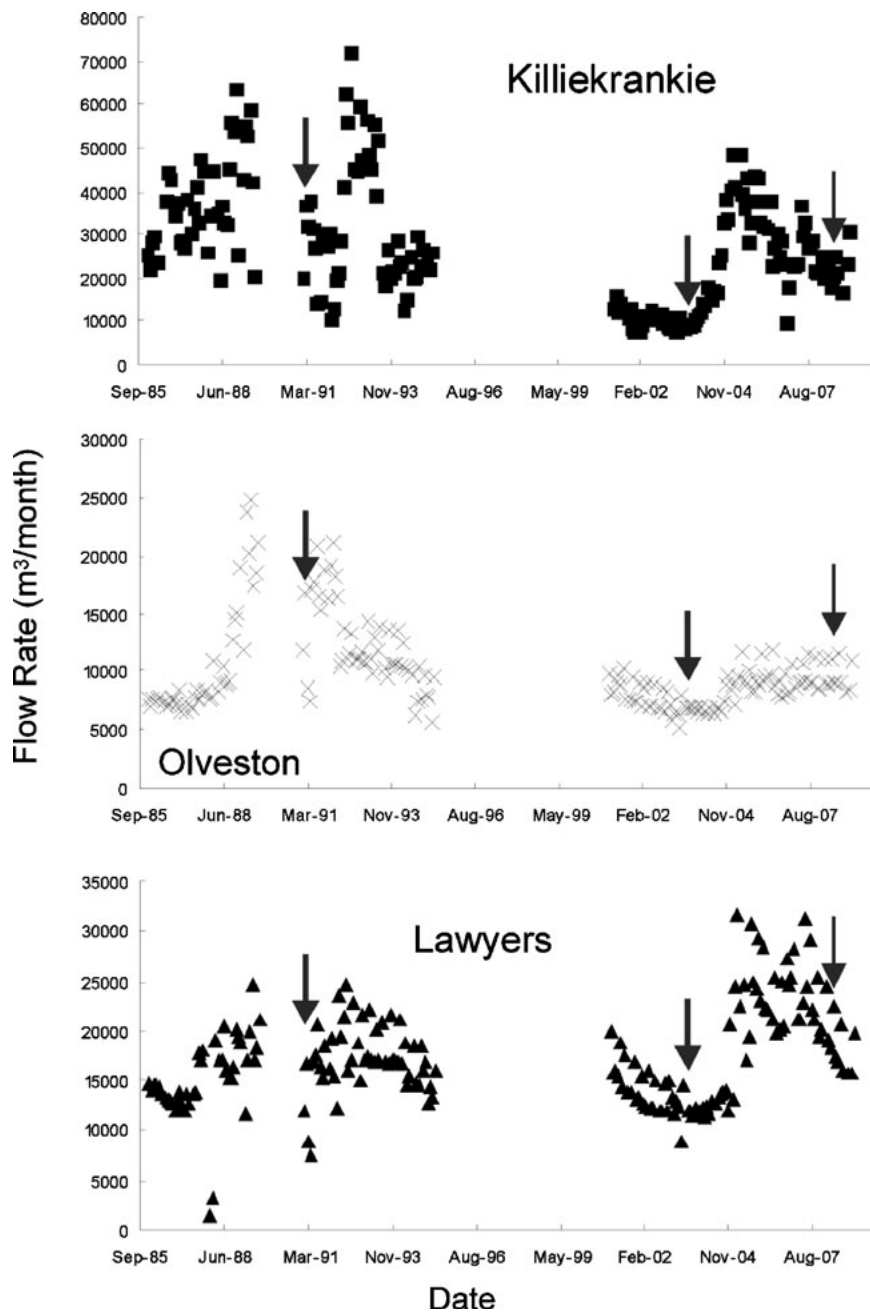


Figure 8

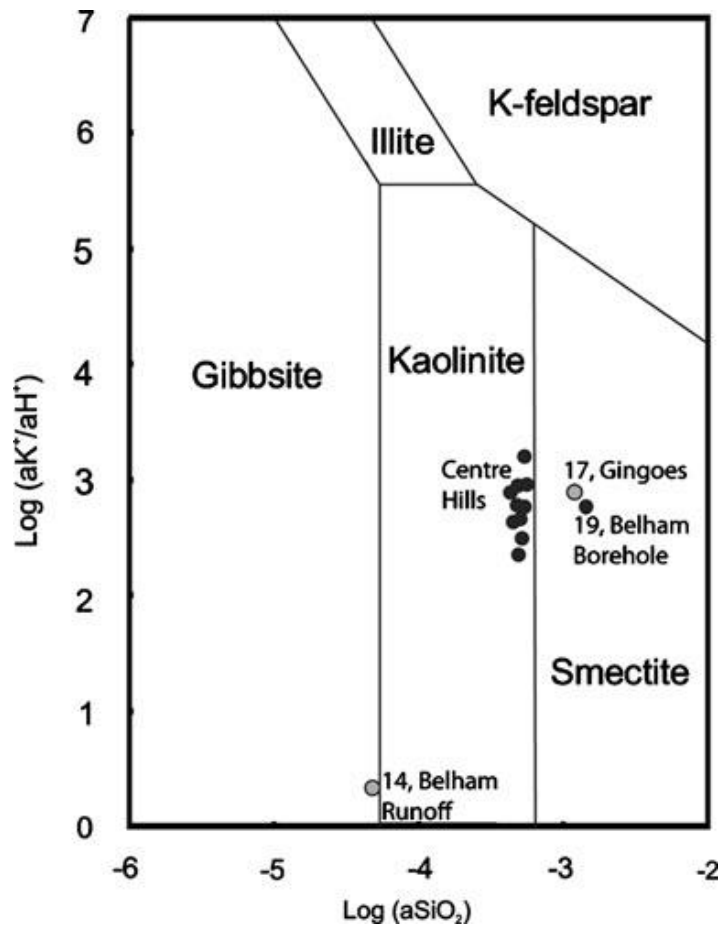


Figure 9

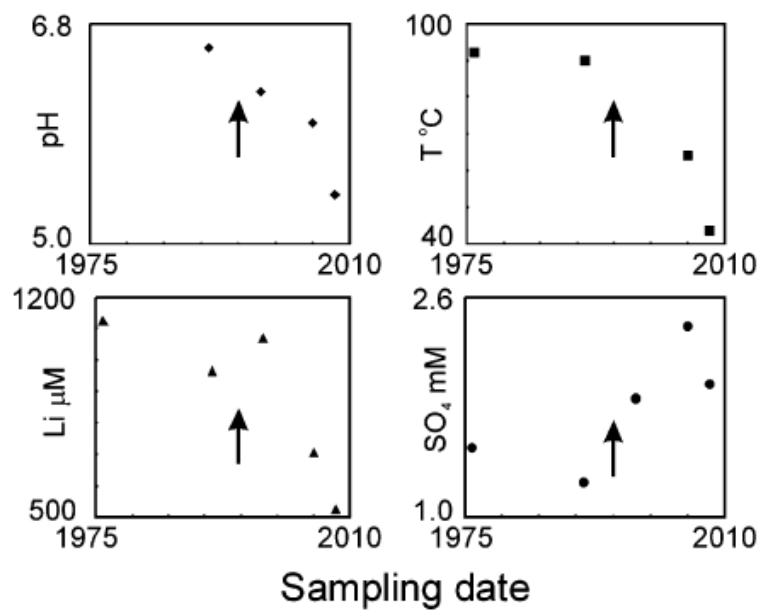


Figure 10

